Allahvirdizadeh, A. and El-Mowafy, A. and Wang, K. 2024. Leveraging Future LEO Constellations for the Precise Orbit Determination of Lower Small Satellites. In: International Technical Meeting of The Institute of Navigation, 23-25 Jan 2024, Long Beach, California.

Leveraging Future LEO Constellations for the Precise Orbit Determination of Lower Small Satellites

Amir Allahvirdi-Zadeh[1], Ahmed El-Mowafy[1], Kan Wang[2]

[1] *School of Earth and Planetary Sciences, Curtin University, GPO Box U1987, Perth, WA 6845, AUSTRALIA*
[2] *National Time Service Center, Chinese Academy of Sciences, Xi'an, China; University of Chinese Academy of Sciences, Beijing, China; Key Laboratory of Time Reference and Applications, Chinese Academy of Sciences, Xi'an, China*

Biographies

Amir Allahvirdi-Zadeh was awarded his PhD in Spatial Sciences from Curtin University, Australia, in 2023. He is a Research Associate at Curtin University, actively engaged in Australian Research Council projects, notably "Next-generation Navigation by Mega-constellations LEO Satellites" and "Tracking formation-flying of nanosatellites using inter-satellite links". He is the developer of the LEO POD modules for the open-source software Ginan.

Ahmed El-Mowafy is a Professor and Director of Graduate Research, the School of Earth and Planetary Sciences, Curtin University, Australia. He obtained his PhD from the University of Calgary, Canada, in 1995 and has more than 230 publications in precise positioning and navigation using GNSS, quality control, POD, integrity monitoring, and estimation theory.

Kan Wang is a Professor at the National Time Service Center, Chinese Academy of Sciences. She received her PhD in GNSS advanced modeling from ETH Zurich in 2016. Her research interests include high-precision GNSS positioning, LEO-augmented PNT service, LEO satellite POD and clock determination, and integrity monitoring.

Abstract

Low earth orbit (LEO) constellations offer possible significant augmentation to the Global Navigation Satellite Systems (GNSS) for positioning, navigation, and timing (PNT) applications. This study explores a new application of forthcoming LEO-PNT constellations; the utilization of signals from higher LEO satellites for precise orbit determination (POD) of lower satellites, such as CubeSats. The integration of LEO-based orbit determination with existing GNSS-based LEO POD methods introduces redundancy and resilience, critical for monitoring the increasingly crowded LEO region in the future. To explore this approach, a simulation is conducted using a constellation of 240 LEO satellites at 1000 km altitude, designed to provide global coverage for the POD of lower satellites. Actual onboard GNSS observations of a 3U CubeSat and its attitude information are employed in a reduced-dynamic POD, generating a true trajectory for the CubeSat. Simulated orbits for the entire constellation and the true trajectory of the CubeSat are used to simulate the navigation signals from the LEO constellation to the CubeSat. Various errors and biases are considered in the simulated observations. To mimic the constraints of limited onboard processing resources, a LEO-PNT module is developed within the new Geoscience Australia's GNSS processing software, Ginan, to process the simulated onboard observations in a Raspberry Pi. The integration of data from higher LEO satellites into the extended Kalman filter model, developed for LEO POD in Ginan, is elucidated and validated through various processing scenarios, including LEO-only case and data fusion with GPS observations. The overall 3D accuracy for the onboard POD is achieved at around 22 cm in the solely LEO-PNT case and improved to about 15 cm with a lower level of observation residuals when combining LEO and GPS observations. This approach holds immense potential for enhancing onboard LEO orbit determination accuracy, robustness, and efficiency.

Keywords: LEO-PNT, onboard CubeSat POD, POD based on EKF, Ginan

 International Technical Meeting of The Institute of Navigation, Long Beach, California, 23 Jan 2024 - 25 Jan 2024.
Proceedings of the 2024 International Technical Meeting of The Institute of Navigation. Institute of Navigation. 756-769. 15 Feb 2024; https://doi.org/10.33012/2024.19485

1 INTRODUCTION

Global navigation satellite systems (GNSS) encounter numerous challenges when operating in critical environments, such as densely populated urban infrastructure, areas with dense foliage, and indoor spaces. A proposed solution utilizes low Earth orbit (LEO) satellites to transmit navigation signals for use in positioning, navigation, and timing (PNT) applications, known as LEO-PNT systems. The LEO-PNT concept originated by leveraging signals from satellites deployed for purposes other than PNT, such as communications, remote sensing, and the Internet of Things. The use of their signal of opportunity (SoP) for PNT is discussed in Kassas et al. (2014) and Khalife et al. (2020). The SoP method involves utilizing measurements of the angle of arrival, signal strength, and Doppler shifts. The achievable accuracy of positioning with SoP is contingent on the chosen method and prevailing conditions. Research findings by Guo et al. (2023) indicate that Doppler positioning using LEO satellite signals can achieve positioning accuracy at the centimeter to decimeter level after solution convergence. Another study by Jardak & Jault (2022) reported a positioning accuracy of 22.7 meters when assuming a known user altitude and tracking up to four LEO satellites. Pinell et al. (2023) recorded an accuracy of 10.5 meters using signals from the Globalstar, Iridium, and Orbcomm constellations. Additionally, Barry & Weiss (2022) mentioned that a LEO satellite positioning error of 0.06 meters can be achieved if a 1 nanosecond range accuracy can be achieved.

In addition to the SoP approach, another viable method for LEO-PNT systems involves broadcasting navigation-ranging signals from a constellation of LEO satellites. The ground segment of this system encompasses tasks such as precise orbit determination and ephemeris computation, clock correction estimation, and periodically updating the satellites with these products. These LEO-PNT systems are tested for various applications, including those requiring precise geodetic solutions, some indoor positioning, and the mitigation of ionospheric and tropospheric effects. The accuracy achievable with LEO-PNT systems ranges from cm-level to dm-level, depending on the techniques and receiver configurations. Examples of these studies are González et al. (2022) and Hong et al. (2023), which demonstrate the growing interest and development of LEO-PNT systems to enhance PNT services.

The upcoming LEO-PNT systems also hold the potential for advancing precise orbit determination (POD) applications, particularly for spacecraft operating within the coverage of LEO-PNT signals. LEO POD utilizing GNSS observations is a technique designed to accurately determine the orbits of satellites in LEO region. This capability is essential for space and Earth science applications, where precise knowledge of a satellite's position is indispensable. Two primary POD methods, namely kinematic and reduced-dynamic approaches, are commonly employed for this purpose, which are usually performed in the post-processing mode. However, real-time onboard POD is crucial for applications requiring immediate orbits such as space navigation, docking and rendezvous, collision avoidance, etc. Onboard POD, particularly for small LEO satellites like CubeSats, is constrained by factors such as satellite power, processing capabilities, and the availability of onboard precise corrections. The latter is no longer a concern with the advent of augmenting free services provided in space such as SouthPAN (https://www.ga.gov.au/scientific-topics/positioning-navigation/positioning-australia/about-the-program/southpan), Japan's QZSS and Galileo's new services, which broadcast precise orbits and clock information through space links. POD based on these space links has been investigated in Allahvirdi-Zadeh et al. (2021) and Hauschild et al. (2022). In addressing the onboard processing limitations, the recent development of the Ginan software (https://geoscienceaustralia.github.io/ginan/page.html) with a filter-based POD module tailored for LEO satellites emerges as a potential solution. Ginan, an open-source GNSS processing advanced software, has been recently developed by Geoscience Australia (GA) and its partners. It is designed to deliver PNT services with a focus on achieving accuracy at the sub-centimeter level. Ginan also provides real-time positioning corrections for precise positioning in diverse scenarios. One of them is the POD of LEO satellites. This capability has been recently developed for Ginan by the GNSS-SPAN group at Curtin University (https://gnss.curtin.edu.au/), enabling both kinematic and reduced-dynamic approaches.

This paper investigates the impact of emerging LEO-PNT navigation signals on the POD of satellites flying at lower altitudes. By evaluating the influence of these signals on the POD process, the research aims to contribute insights into enhancing the accuracy and reliability of the onboard spacecraft orbit determination in LEO. Following this introduction, the paper initiates by simulating a LEO-PNT constellation, intended for use in the POD of a lower satellite. Subsequently, the paper proceeds to establish the requisite reference orbit using the reduced-dynamic POD of an actual CubeSat. This orbit serves as a reference to generate observations from the LEO-PNT constellation to the CubeSats. The kinematic POD model based on the extended Kalman filter (EKF) approach is then developed and implemented in Ginan. The ensuing section discusses the outcomes of the combined LEO POD, providing insights into the effectiveness of this approach. The paper concludes with a summary of key findings and their implications.

2 SIMULATING LEO-PNT CONSTELLATION

Simulating a LEO-PNT constellation requires a comprehensive consideration of various factors to accurately model the system's performance. For instance, the satellites' altitude significantly influences the orbital period and ground coverage. Equally critical is the orbital plane inclination, impacting ground coverage, revisit time, launch requirements, mission costs, satellite visibility,

 International Technical Meeting of The Institute of Navigation, Long Beach, California, 23 Jan 2024 - 25 Jan 2024.
Proceedings of the 2024 International Technical Meeting of The Institute of Navigation. Institute of Navigation. 756-769. 15 Feb 2024; https://doi.org/10.33012/2024.19485

sunlight exposure, and orbital stability. Other crucial factors come into play to ensure a realistic portrayal of anticipated errors in PNT solutions. These encompass satellite dynamics, characteristics of PNT signals and antennas, the ground segment, onboard clocks, data downlink and uplink processes, as well as error models. Ongoing research and development efforts are dedicated to exploring these multifaceted elements. Nevertheless, an exhaustive discussion of all these factors is beyond the scope of this study.

The constraints of LEO-PNT systems concerning coverage involve maintaining a minimum number of satellites and orbital planes for achieving global coverage. Simulations, as detailed in the study by Prol et al. (2022), indicated that altitudes ranging from 500 to 1000 km are viable regions for deploying LEO satellites. Within this range, a reasonable balance is struck between mitigating path losses and contending with drag forces induced by Earth's gravity. While higher altitudes theoretically offer improved coverage, the distribution reveals an asymptotic pattern. Beyond the 1000 km threshold, to a few hundreds of kilometers, the simulations demonstrate a diminishing return, with no significant enhancements in the number of satellites and planes obtained.

Among various constellation design models, the Walker delta model, also known as the Ballard rosette, is commonly favored for navigation systems due to its ability to maintain symmetric coverage by users on the ground. The constellation designed using the Walker delta model exhibits uniform orbits, eccentricity, and inclination. This design ensures that any perturbations comparably affect each satellite, thereby preserving the geometric arrangement. Consequently, this minimizes the need for excessive station-keeping maneuvers and reduces overall fuel usage.

The walker-delta pattern is represented as $I: T/P/F$, where I denotes the inclination, T signifies the total number of satellites, P represents the number of equally spaced orbital planes, and F indicates the interplane phase increment. A simulation of a constellation comprising 240 LEO satellites positioned at an altitude of 1000 km in a near-polar orbit has been conducted utilizing the Walker Delta model. The specific configuration of this constellation is denoted by the pattern 85.64°: 240/12/6. This arrangement is designed to enable the observation of 6-7 satellites simultaneously across most regions on Earth. Such a configuration proves highly advantageous for positioning and navigation applications, as detailed in the study by El-Mowafy et al. (2023). The right ascension of the ascending nodes (Ω) and the mean anomaly (M) of the satellite j on plane i are calculated as follows (Guan et al., 2020):

$$\begin{aligned} \Omega_{ij} &= \frac{2\pi}{P}(i-1) \\ M_{ij} &= \frac{2\pi P}{T}(j-1) + \frac{2\pi}{T}F(i-1) \end{aligned} \tag{1}$$

Figure 1 illustrates a one-sided view of the distribution of satellites within the constellation.

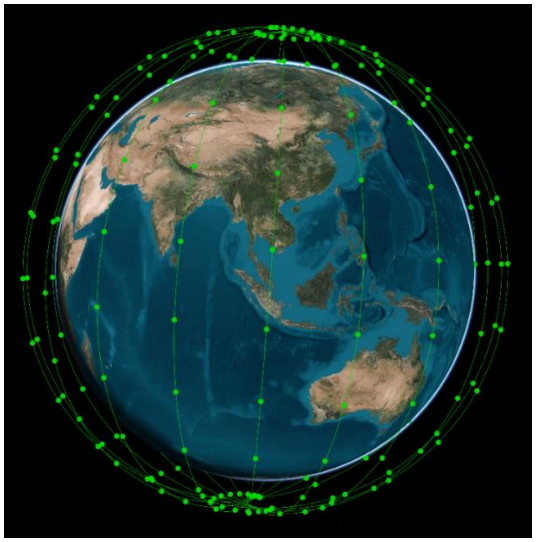

FIGURE 1
Simulated LEO constellation

 International Technical Meeting of The Institute of Navigation, Long Beach, California, 23 Jan 2024 - 25 Jan 2024. Proceedings of the 2024 International Technical Meeting of The Institute of Navigation. Institute of Navigation. 756-769. 15 Feb 2024; https://doi.org/10.33012/2024.19485

3 SIMULATING LEO-PNT OBSERVATIONS

This section delves into the simulation of observations from the LEO constellation, discussed in the preceding section, to a CubeSat. To achieve this, the reduced-dynamic POD is employed to ascertain the precise orbit of the evaluated CubeSat, which serves as the reference orbit. The reference orbit, coupled with the actual attitude of the CubeSats, is compared with the simulated orbits of the constellation to validate the simulation of LEO-PNT observations. The subsequent section further elaborates on this simulation process.

3.1 Reduced-Dynamic POD of CubeSat

A 3U-CubeSat from the Spire constellation (https://spire.com) is selected as the testing satellite for this study (Figure 2). Despite its orbit from the mission provider being available, it was not used for data simulation for two reasons. Firstly, these CubeSats lack satellite laser ranging reflectors, rendering external validation of estimated orbits unfeasible. Secondly, the provided orbits exhibit long sample intervals (1 minute), and the 3D root mean square (RMS) values of these orbits are reported to be worse than 27 cm and 0.32 mm/s (Arnold et al., 2023). Additionally, there is a lack of information regarding internal POD validation metrics, such as observation residuals. Therefore, the provided orbits do not align with the requirements of this study. To address these limitations, a comprehensive reduced-dynamic POD using Bernese GNSS software (Dach et al., 2015) has been meticulously executed based on 3 hours of onboard observations from 20:00 to 23:00 UTC on 21 June 2023. This process aims to derive 1-Hz precise orbits, subsequently referred to as the "reference orbit," specifically tailored to meet the demands of this study.
The detailed procedure for the reduced-dynamic POD of the LEO satellites, including the estimation model, is thoroughly explained in Allahvirdi-Zadeh & Wang et al. (2022) and Wang et al. (2020). The POD specifications for the tested CubeSat are outlined in Table 1. These orbits have been rigorously validated, demonstrating 3D RMS value of less than 10 cm and phase observation residuals deemed acceptable at less than 1 cm for daily observations. This validation has been consistently confirmed across various studies (Allahvirdi-Zadeh & El-Mowafy, 2022a; Allahvirdizadeh, 2022; Arnold et al., 2023). Additional details of the tested CubeSat are outlined in Table 1.

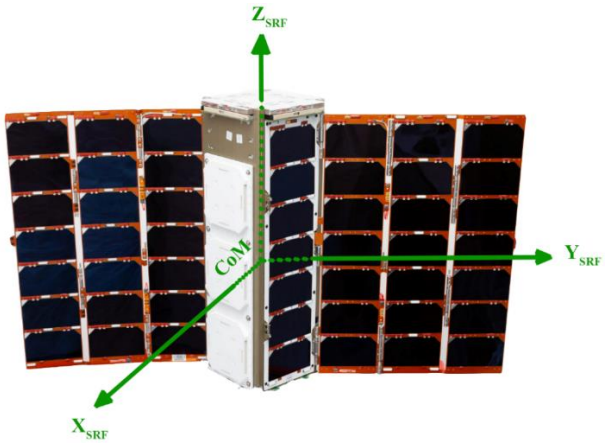

FIGURE 2
CubeSat structure with satellite reference frame representation

 International Technical Meeting of The Institute of Navigation, Long Beach, California, 23 Jan 2024 - 25 Jan 2024. Proceedings of the 2024 International Technical Meeting of The Institute of Navigation. Institute of Navigation. 756-769. 15 Feb 2024; https://doi.org/10.33012/2024.19485

TABLE 1

Reduced-dynamic POD specifications

Item	Description
Dynamic models and Stochastic accelerations	Gravity field: Earth gravitational model (EGM 2008) (Pavlis et al., 2008)
	Tidal corrections: Finite element solution tidal model – FES2014b (Carrere et al., 2015)
	Relativity: IERS 2010 (Petit & Luzum, 2010)
	Planets ephemeris: JPL DE421 (Folkner et al., 2009)
	Velocity changes (pulses) and piece-wise constant accelerations (Jäggi et al., 2006)
Observation model	Observations model: Ionospheric-free linear combination of 1 Hz GPS code (C1, C2) and phase (L1, L2) Stochastic model: SNR-based weighting model (Allahvirdi-Zadeh, El-Mowafy, et al., 2022)
	Eclipsed observations: Removed using the shadow model (Allahverdi-Zadeh et al., 2016)
	Code and phase standard deviation: 0.5 m and 5 mm
	Satellite attitude information: Obtained as quaternions
	Phase ambiguities: Fixed by applying observable-specific signal biases (OSB) from center for orbit determination in Europe (CODE) (Schaer et al., 2021)
CubeSat specification	CubeSat ID: L172 – Mass: 4.6 kg – Area (front panel): 0.03 m2 – altitude: ~540 km – Orbit Type: Sun-Sync
	Satellite reference frame (SRF) of CubeSat: Origin: center of mass (CoM) X_{SRF} : FRO antenna side (~ +velocity direction) Y_{SRF} : Completes right-handed triple (X × Y = Z) Z_{SRF} : Narrow end of spacecraft, opposite the POD antenna
	Antenna boresight: [0, 0, -1] Antenna azimuth: [+1, 0, 0] Antenna sensor offset: [-0.0047, 0.0024, -0.1631] m Antenna PCO: [0.0021, 0.0011, -0.0223] m for L1 [0.0033, 0.0034, -0.0125] m for L2 Empirical phase center variation (PCV) maps (Allahvirdi-Zadeh, 2021)

The residuals of reduced-dynamic POD for the ionospheric-free phase observations of all GPS satellites on the testing date are illustrated in Figure 3. Most residuals exhibit a magnitude of less than 4 cm, with an overall RMS of approximately 1.7 cm. The 95% upper and lower bounds are depicted in the figure and mostly ranged within ±3.5 cm.

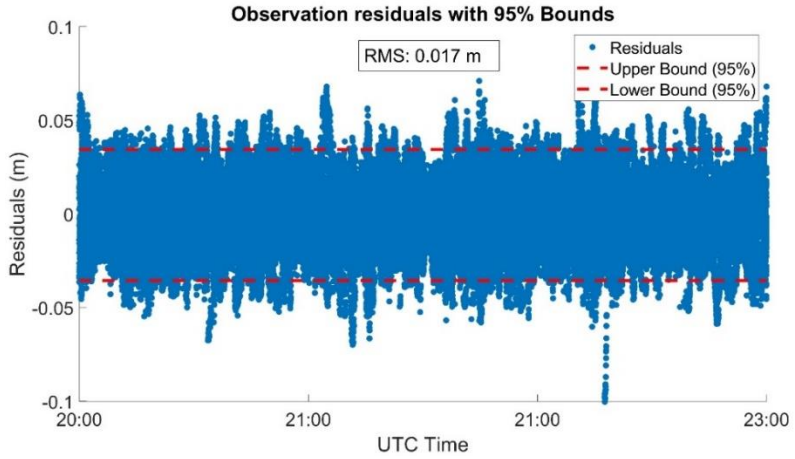

FIGURE 3

Observations residuals of reduced-dynamic POD for the testing CubeSat

 International Technical Meeting of The Institute of Navigation, Long Beach, California, 23 Jan 2024 - 25 Jan 2024. Proceedings of the 2024 International Technical Meeting of The Institute of Navigation. Institute of Navigation. 756-769. 15 Feb 2024; https://doi.org/10.33012/2024.19485

3.2 LEO-PNT Observation Models

In this section, simulations are conducted to generate observations from the LEO-PNT constellation to the CubeSat. To simulate observations for the CubeSat under examination, the previously estimated reference CubeSat orbit, denoted as r_{Ref}, and the attitude matrix from the onboard attitude determination and control system (ADCS) of the CubeSat (R_0) are employed to represent the true trajectory of the CubeSat. The orbits of the simulated LEO constellations (r^s_{cstl}) in the Earth-centered Earth-fixed (ECEF) frame are derived from the Walker delta model. To accommodate ionospheric delays ($i^s_{r,f}$) for frequency f, the following spacecraft ionospheric model is applied (Spirent, 2022):

$$i^s_{r,f} = \frac{82.1 \times TEC}{f^2\left(\sqrt{\sin^2 e + 0.076} + \sin e\right)} \tag{2}$$

where TEC represents the total electron content, and e denotes the elevation angle of the GNSS satellite to the CubeSat. This ionospheric model considers the decrease in ionization levels, with increasing height in the ionospheric layer. Equation 2 is directly applicable only for positive elevation angles. For negative satellite elevations, the ionospheric delay is calculated by assuming symmetrical deviation for signal paths that fully traverse the ionosphere. The net delay is computed as the value applicable in this scenario, subtracting the delay obtained for the corresponding positive elevation at the CubeSat's position. The initial TEC value is treated as a constant (10^{17} electrons/m^2) for this simulation. While it is feasible to introduce positional and sinusoidal variations, these have been omitted for the sake of simplicity. The observation simulation accounts for antenna phase center offsets (PCO) provided by the Spire team (see Table 1). To simulate onboard multipath for the CubeSat's antenna, empirical PCV maps, derived using a residual approach over an extended period of actual data, as outlined in Allahvirdi-Zadeh (2021), are integrated into the simulation. Comparable noise levels to those considered for the reduced-dynamic POD for the raw observations (specified in Table 1) are applied in the simulation. The combined effects of these noises and multipath errors are denoted as ε_p and ε_φ for code and phase observations, respectively.

As the receiver clock error is assumed to be estimated epoch-wise in the POD processes (Allahvirdi-Zadeh & Wang et al., 2022) without applying any receiver clock model, this estimation remains independent of the simulated LEO satellite clocks. It is thus set to zero in this context. The simulation method of receiver clocks becomes pertinent when a receiver clock model is applied during the estimation (Wang & El-Mowafy, 2020, 2021), a practice not recommended for CubeSats due to the substantial systematic effects in their onboard oscillators. Further details on the instabilities in CubeSats' clocks are provided in Allahvirdi-Zadeh & Awange et al. (2022).

These specifications enable us to simulate 1-Hz observations tailored explicitly for the tested CubeSat as follows:

$$\begin{aligned} p^s_{r,f} &= \left\|\left(r_{Ref} + TR_0 r_i\right) - r^s_{cstl}\right\| + i^s_{r,f} + \varepsilon_p \\ \varphi^s_{r,f} &= \left\|\left(r_{Ref} + TR_0 r_i\right) - r^s_{cstl}\right\| - i^s_{r,f} + \lambda_f n^s_{r,f} + \varepsilon_\varphi \end{aligned} \tag{3}$$

Here, r_i represents the coordinates of the antenna in SRF, provided in Table 1, transformed from the inertial frame into the ECEF frame using the transformation T and attitude R_0 matrices. For simplicity, all hardware biases and clock errors are considered zeros. The phase ambiguity parameter $n^s_{r,f}$ is transformed from cycles to the range scale by multiplying it by the wavelength λ_f.

Due to the high dynamics of LEO satellites and the lower altitude of the CubeSat, the CubeSat enjoys excellent coverage. Considering no elevation mask angle, the number of tracked LEO satellites from the constellation during the testing period has consistently been no less than 19 satellites and peaked at 59 simultaneously tracked satellites. Figure 4 illustrates the distribution of the number of tracked LEO satellites by the tested CubeSat. The vertical axis, labelled as "Frequency", represents the total number of epochs for the associated number of satellites in the horizontal axis. During the simulation time (3 hours of 1 Hz observations), 22 LEO satellites were available in over 1000 epochs. The carrier phase observations for these satellites are also shown in Figure 5.

 International Technical Meeting of The Institute of Navigation, Long Beach, California, 23 Jan 2024 - 25 Jan 2024. Proceedings of the 2024 International Technical Meeting of The Institute of Navigation. Institute of Navigation. 756-769. 15 Feb 2024; https://doi.org/10.33012/2024.19485

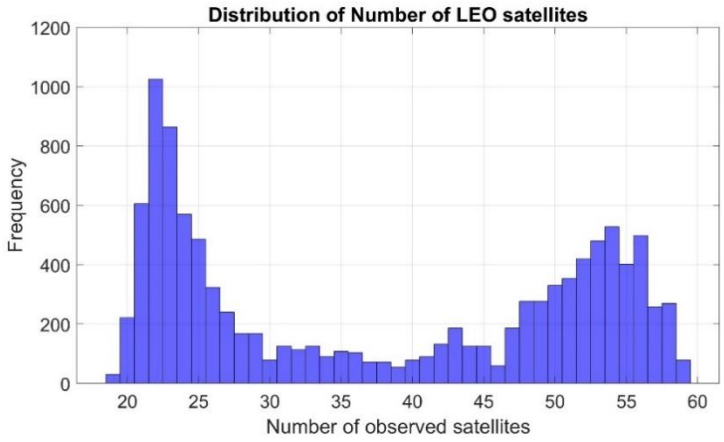

FIGURE 4
Distribution of the number of tracked LEO satellites by the CubeSat

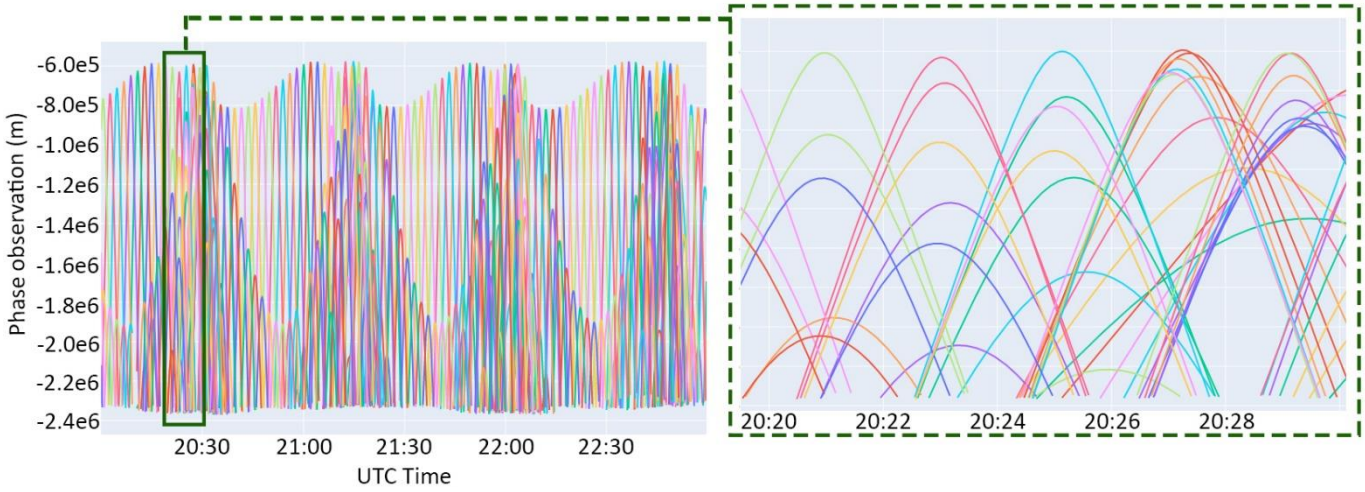

FIGURE 5
Phase Observations for the LEO Constellations – Each satellite's observation is represented by a distinct color.

As mentioned in Equation (3) and presented in Table 1, the simulation incorporates attitude quaternions as well as antenna boresight and azimuth directions. Figure 6 displays the elevation angles of the simulated satellites ranging from 0 to 90 degrees, highlighting the accurate consideration of satellite orientation in space during the simulation. POD using these simulated observations is discussed in the following section.

 International Technical Meeting of The Institute of Navigation, Long Beach, California, 23 Jan 2024 - 25 Jan 2024. Proceedings of the 2024 International Technical Meeting of The Institute of Navigation. Institute of Navigation. 756-769. 15 Feb 2024; https://doi.org/10.33012/2024.19485

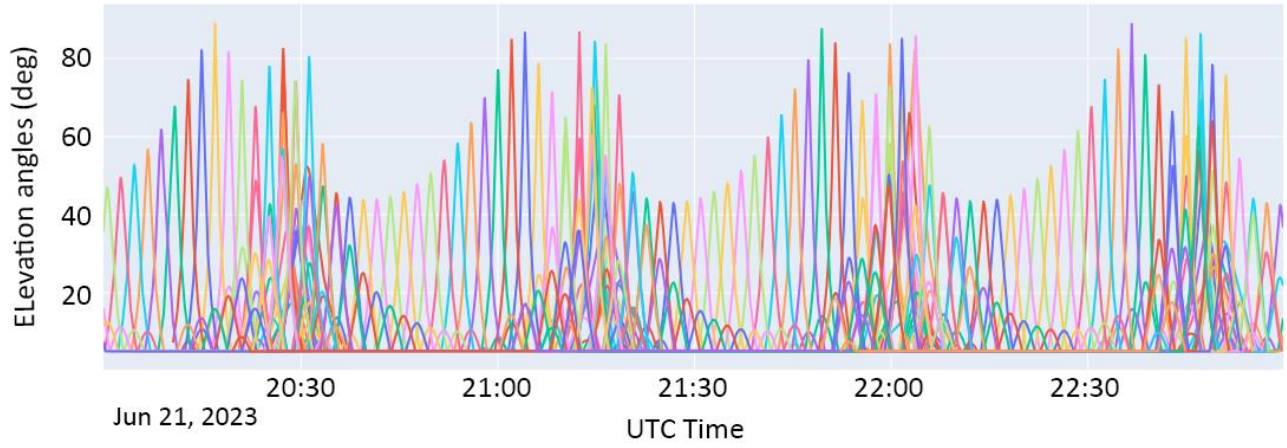

FIGURE 6
Elevation angles of the LEO constellation observed at the testing CubeSat- Each satellite's elevation angle is represented by a distinct color.

4 KINEMATIC POD IN GINAN

In this section, the necessary model for processing the simulated LEO-PNT observations is presented. These models are implemented within an EKF using the Ginan processing software. Considering all observations of m LEO-PNT satellites at epoch t in $y_t = [P \quad \Phi]^T$, where $P = \left[P_{r,1}^T, \dots, P_{r,f}^T\right]$ and $\Phi = \left[\Phi_{r,1}^T, \dots, \Phi_{r,f}^T\right]$ represent the observations for frequencies 1 to f, with each element defined as $P_{r,f} = \left[p_{r,f}^1, \dots, p_{r,f}^m\right]^T$ and $\Phi_{r,f} = \left[\varphi_{r,f}^1, \dots, \varphi_{r,f}^m\right]^T$ for arbitrary frequency f and with m denoting the number of used GNSS satellites, the observation model is formed as follows:

$$E(y_t) = A_t x_t + \varepsilon_t \tag{4}$$

Here, $E(.)$ represents the expected value, A_t is the design matrix containing the partial derivatives of the observations with respect to the unknown parameters in the state vector x_t, and ε contains the remaining errors. The state vector $x = \left[r^T, \dot{r}^T, dt_r, \dot{dt}_r, n^T, i_{STEC}^T\right]^T$ for the kinematic POD comprises the position (r) and position rate or velocity ($\dot{r}$) of the CubeSat, the onboard receiver clock offset error (dt) and its rate ($\dot{dt}$), ambiguities (n), and ionospheric slant total electron content (i_{STEC}), which is estimated with the between-epoch variations considered in the next steps of time updates. Due to the omission of modelling the CubeSat clock error in the simulation step, the time update steps do not involve the onboard receiver clock error and its drift.
The covariance matrix of the system noise is generated using the random walk model and the state transition matrix (STM) F_t is simplified to the identity matrix ($F_t = \mathbf{1}$), except for states with rate terms, such as position (and CubeSat clock in general POD case), where the specific structure of the STM matrix is given by:

$$F_t = \begin{bmatrix} 1 & \delta t \\ 0 & 1 \end{bmatrix} \tag{5}$$

where δt represents the time difference between two consecutive epochs. This structure for the STM indicates that the previous state contributes directly to the current state, and the zeros in the off-diagonal elements signify that the influence of the process noise variance matrix is dominant. Table 2 provides the a-priori values for the standard deviation and process noise in the filter.

Concerning the integration of LEO-PNT observations with other constellations, for the sake of simulation simplicity, the simulated observations for the LEO-PNT constellation adopt signal characteristics similar to GPS satellites. As a result, there is no requirement to account for inter-system biases (ISB) in this study. The exploration of more complex models, including signals with different characteristics and the implementation of other GNSS, will be part of our future work.

 International Technical Meeting of The Institute of Navigation, Long Beach, California, 23 Jan 2024 - 25 Jan 2024. Proceedings of the 2024 International Technical Meeting of The Institute of Navigation. Institute of Navigation. 756-769. 15 Feb 2024; https://doi.org/10.33012/2024.19485

TABLE 2

Initial values for the state vector in the EKF in Ginan

State	Standard deviation ($\boldsymbol{\sigma}$)	Process noise
Position	30 m	0 m
Position rate (velocity)	5000 m/s	1000 m/s
Ambiguity	6000 m	0 m
Ionosphere slant TEC	1000 m	8000 m

5 RESULTS AND DISCUSSION

In this section, we explore the kinematic POD of the tested CubeSats utilizing LEO-PNT observations. In order to replicate the onboard processing constraints, Ginan has been compiled on a Raspberry Pi 4 equipped with ARM CPU v8 for POD processing, as illustrated in Figure 7. This further validates the high performance of Ginan in constraint processing units, instilling confidence in the prospect of compiling Ginan for actual onboard POD. In terms of the processing time, each epoch requires less than 1 second for completion.

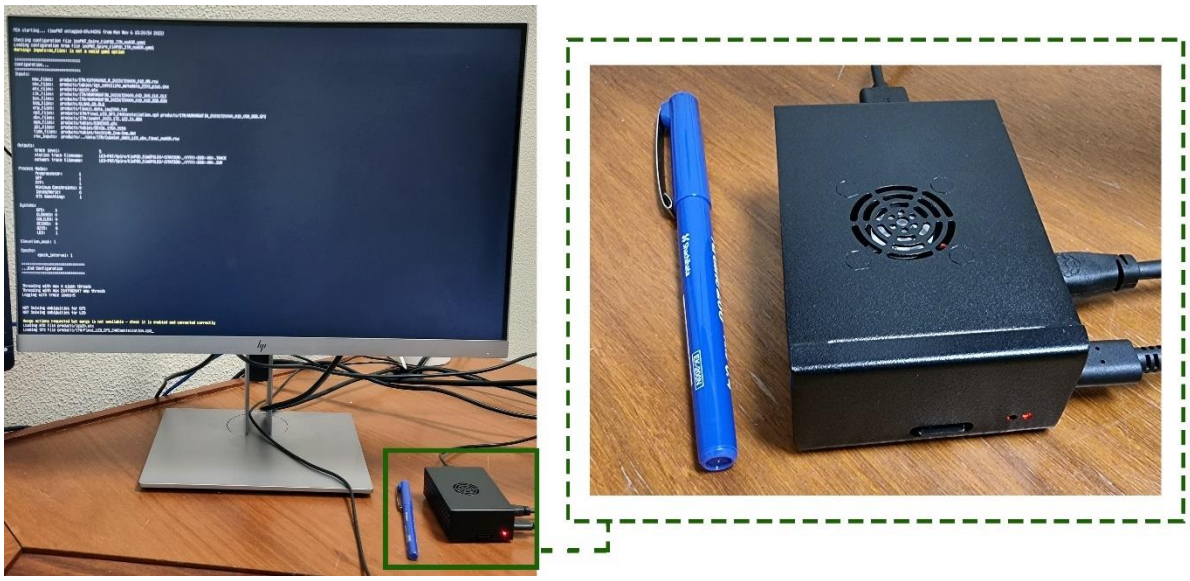

FIGURE 7

Raspberry Pi and the compiled Ginan on Ubuntu server 20.04.

To investigate the achievable POD accuracy using a LEO-PNT, the initial processing scenario involves conducting CubeSat POD solely based on simulated LEO-PNT observations. The phase observation residuals for all satellites in this scenario are presented in Figure 8 to demonstrate the best-fitting of the model. With the exception of the initial epochs, where initialization effects are evident, the residuals for all LEO-PNT satellites consistently exhibit RMS values better than 6 mm. This internal consistency validates the efficacy of the kinematic POD using solely LEO-PNT observations.

 International Technical Meeting of The Institute of Navigation, Long Beach, California, 23 Jan 2024 - 25 Jan 2024. Proceedings of the 2024 International Technical Meeting of The Institute of Navigation. Institute of Navigation. 756-769. 15 Feb 2024; https://doi.org/10.33012/2024.19485

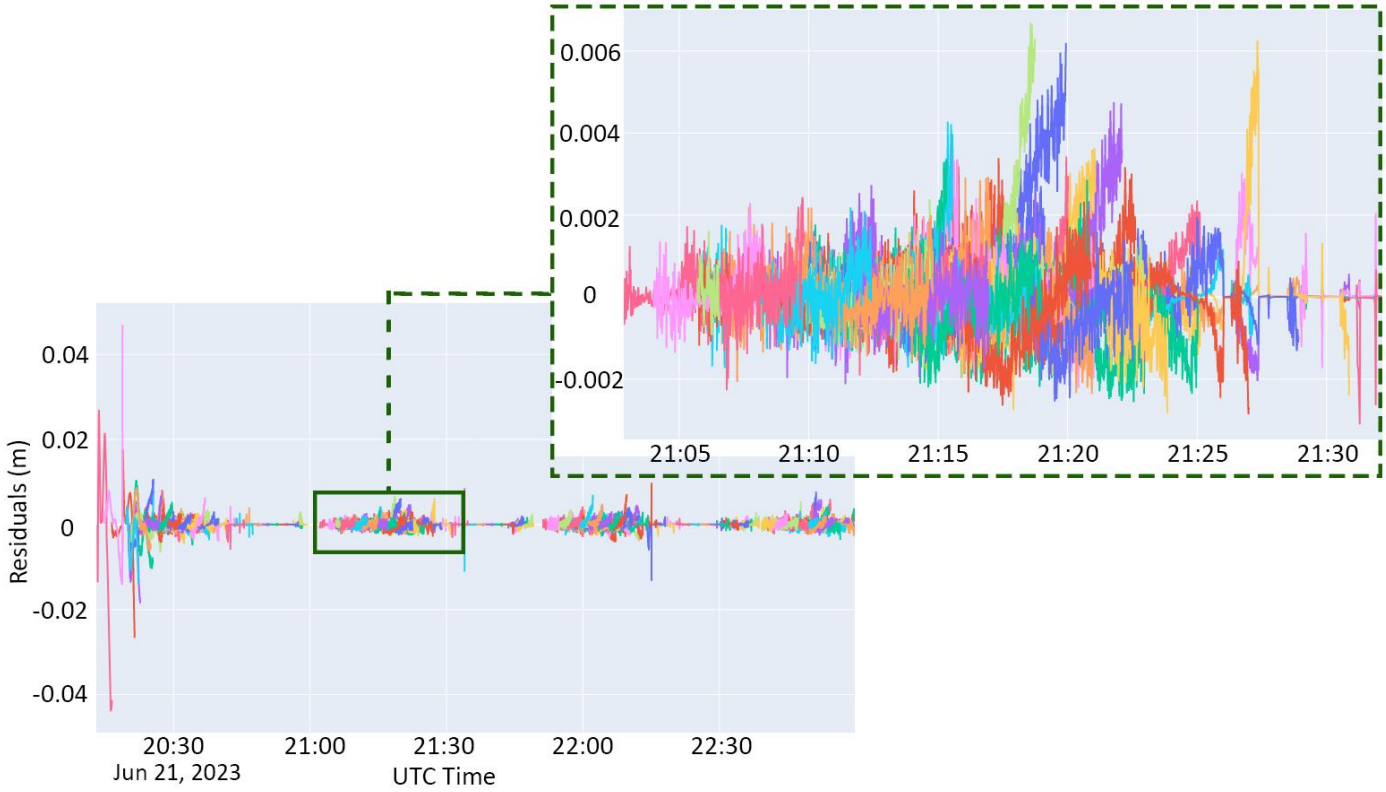

FIGURE 8

Residuals of phase observations for kinematic CubeSat POD based on only LEO-PNT observations – Each satellite's observation residual is presented by a distinct color

Upon comparison with the reference orbits, the kinematic POD relying solely on LEO-PNT observations exhibits root mean squared error (RMSE) values better than 30 cm across the three orbital components, as detailed in Table 3. Only 3% of this comparative analysis reveals values exceeding 1 meter compared to the reference orbits. Notably, these instances are primarily associated with the initialization of the filter in Ginan. As such, they have been excluded from the RMSE calculation and marked as outliers in the table.

TABLE 3

*RMSE of kinematic POD based on only LEO-PNT observations – * Outliers are epochs excluded due to having differences exceeding 1 meter*

RMSE X (m)	RMSE Y (m)	RMSE Z (m)	3D RMSE (m)	Outlier* (%)
0.26	0.17	0.22	0.22	3

In the second scenario, LEO POD is conducted by combining both GPS and LEO-PNT observations. The objective of this scenario is to explore the feasibility of incorporating both constellations in the onboard CubeSat POD and assess the potential improvement in POD accuracy when augmenting GPS by LEO observations. Considering that technological advancements will likely overcome limitations in the number of channels for onboard receivers. Figure 9 depicts the number of observed satellites from both constellations. Comparing the figure with Figure 4 shows that the number of available satellites reaches 72 satellites. In Figures 4 and 9, no elevation mask angle has been applied to represent all available satellites, even those with negative elevation angles. Receiving signals from negative elevation angles could be valuable for attitude determination, especially if the CubeSat is equipped with an array of antennae, as presented in Allahvirdi-Zadeh & El-Mowafy (2022b). Processing time with Ginan for each epoch was below 1 second.

 International Technical Meeting of The Institute of Navigation, Long Beach, California, 23 Jan 2024 - 25 Jan 2024. Proceedings of the 2024 International Technical Meeting of The Institute of Navigation. Institute of Navigation. 756-769. 15 Feb 2024; https://doi.org/10.33012/2024.19485

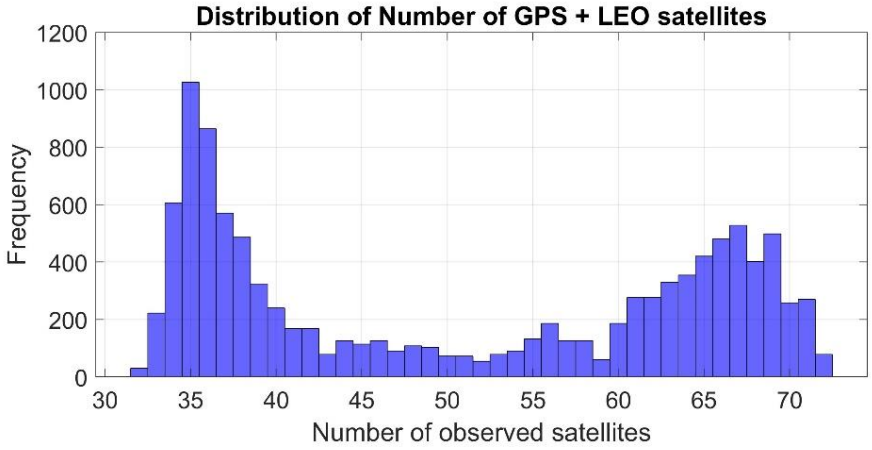

FIGURE 9
Distribution of the number of tracked GPS + LEO satellites by the CubeSat

The phase observation residuals have significantly improved in the GPS+LEO scenario, reaching values better than 3 mm, as illustrated in Figure 10. The RMSE values for the discrepancies between the reference orbit and the kinematic POD have improved. As highlighted in Table 4, the 3D RMS of the orbital components is around 15 cm, with less than 1% outliers observed in this comparison. Achieving decimeter-level accuracy for onboard POD is crucial for many real-time applications. This level of precision is indispensable for Earth observation missions, geocoding, autonomous instrument and spacecraft operations, as well as autonomously controlling orbital motions.

TABLE 4

RMSE of kinematic POD based on combining GPS and LEO-PNT observations

RMSE X (m)	RMSE Y (m)	RMSE Z (m)	3D RMSE (m)	Outlier (%)
0.15	0.12	0.18	0.15	< 1

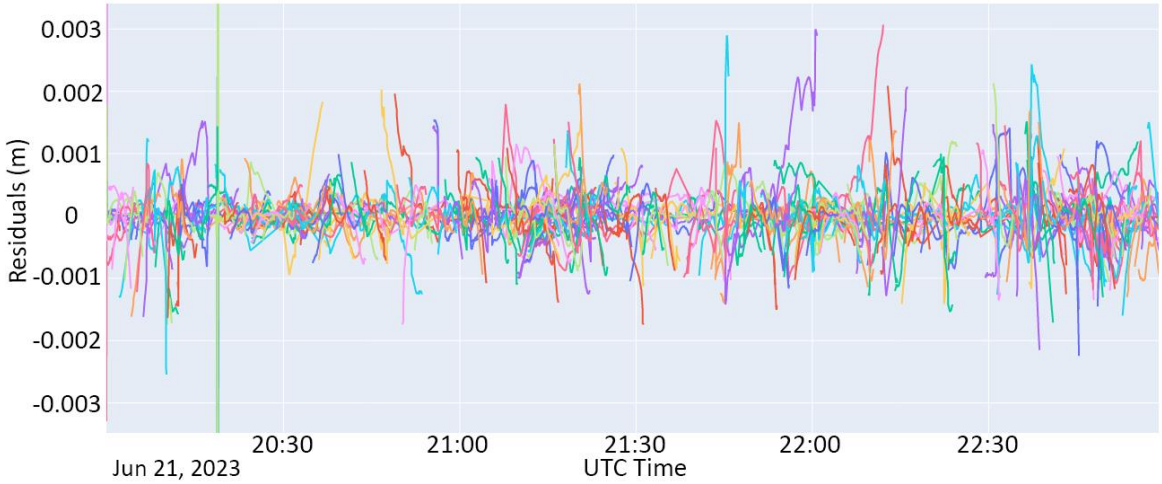

FIGURE 10
Residuals of phase observations for kinematic CubeSat POD based on combined GPS and LEO-PNT observations

 International Technical Meeting of The Institute of Navigation, Long Beach, California, 23 Jan 2024 - 25 Jan 2024. Proceedings of the 2024 International Technical Meeting of The Institute of Navigation. Institute of Navigation. 756-769. 15 Feb 2024; https://doi.org/10.33012/2024.19485

To highlight the advantages of LEO-PNT systems for CubeSat POD, the testing scenarios have been compared with the kinematic POD relying solely on GPS observations, as detailed in Table 5. Utilizing LEO-PNT for POD serves as a robust backup in instances where the GNSS receiver encounters malfunctions. The incorporation of LEO data to the GPS-only scenario introduces additional observations, leading to an enhancement of approximately 12% in the 3D orbital accuracy of GPS.

TABLE 5

Comparing the kinematic POD results

Processing case	RMSE X (m)	RMSE Y (m)	RMSE Z (m)	3D RMSE (m)	Outlier (%)
LEO-PNT	0.26	0.17	0.22	0.22	3
GPS	0.18	0.15	0.19	0.17	1.7
GPS + LEO-PNT	0.15	0.12	0.18	0.15	< 1

6 CONCLUSION

The upcoming LEO constellation is anticipated to provide a greater number of observations to support satellite-based PNT with enhanced reliability, particularly in high-density areas such as urban canyons and some indoor environments. This presents an opportunity for POD of small satellites orbiting at lower altitudes within the LEO-based PNT constellation. This study investigates this scenario for POD of an actual CubeSat flying at an altitude of approximately 500 km. Utilizing the Walker Delta model, a constellation of 240 satellites distributed across 12 orbital planes at an altitude of 1000 km was simulated. Onboard observations at the tested CubeSat were processed using a comprehensive reduced-dynamic POD to generate a reference orbit. This reference orbit, coupled with attitude quaternions, was employed along with the orbital information of the simulated constellation and requisite models to simulate observations from LEO systems for the positioning of the CubeSat. The maximum number of satellites that was tracked by the CubeSat ranged from 59 in the case of solely LEO-PNT satellites to 72 when considering both GPS and LEO constellations.

The EKF-based LEO POD modules developed within the Australian Ginan processing software were compiled on a Raspberry Pi to emulate onboard processing situations. Processing of each epoch requires less than 1 second. The CubeSat's kinematic POD was validated by comparison with the reference orbit, showing a 3D RMSE of 22 cm for the LEO-PNT case. This highlights the potential of the LEO-PNT system as a backup for GPS in the event of a GNSS receiver malfunction. The orbital accuracy improved to 15 cm when GPS data was combined with LEO constellations, which is approximately 12% better than kinematic POD utilizing only GPS observations. Internal validations indicated phase residuals better than 6 mm for the LEO PNT case, which is reduced to around 3 mm when considering both GPS and LEO observations. These results demonstrate the potential benefits of future LEO-PNT constellations for POD of small LEO satellites, including CubeSats, in lower altitudes, and the robust performance of Ginan for onboard POD applications.

ACKNOWLEDGMENTS

The authors would like to express their gratitude to Spirent for providing access to the SimGEN software, which helped in simulating and evaluating various scenarios throughout this research. Additionally, the authors would like to acknowledge LEAP Australia for providing access to the Ansys Satellite Tool Kit (Ansys STK) for the LEO-PNT simulation. Special thanks to Spire Global Inc. for providing the nanosatellite data for scientific research. Geoscience Australia is highly acknowledged for developing Ginan software. Funding of this research work by the Australian Research Council under the Discovery Project DP240101710 is acknowledged.

REFERENCES

Allahverdi-Zadeh, A., Asgari, J., & Amiri-Simkooei, A. R. (2016). Investigation of GPS draconitic year effect on GPS time series of eliminated eclipsing GPS satellite data. *Journal of Geodetic Science*, *6*(1), 93-102. https://doi.org/10.1515/jogs-2016-0007

Allahvirdi-Zadeh, A. (2021, 25 November 2021). Phase centre variation of the GNSS antenna onboard the CubeSats and its impact on precise orbit determination. GSA Earth Sciences Student Symposium, Western Australia (GESSS-WA), Perth, Australia. https://doi.org/10.13140/RG.2.2.10355.45607/1

 International Technical Meeting of The Institute of Navigation, Long Beach, California, 23 Jan 2024 - 25 Jan 2024. Proceedings of the 2024 International Technical Meeting of The Institute of Navigation. Institute of Navigation. 756-769. 15 Feb 2024; https://doi.org/10.33012/2024.19485

Allahvirdi-Zadeh, A., Wang, K., & El-Mowafy, A. (2021). POD of small LEO satellites based on precise real-time MADOCA and SBAS-aided PPP corrections. *GPS solutions*, *25*(31), 1-14. https://doi.org/10.1007/s10291-020-01078-8
Allahvirdizadeh, A. (2022). *Precise Orbit Determination of CubeSats* [Thesis by publication, Curtin University]. Curtin Theses. http://hdl.handle.net/20.500.11937/89922
Allahvirdi-Zadeh, A., Awange, J., El-Mowafy, A., Ding, T., & Wang, K. (2022). Stability of CubeSat Clocks and Their Impacts on GNSS Radio Occultation. *Remote Sensing*, *14*(2), 1-26. https://doi.org/10.3390/rs14020362
Allahvirdi-Zadeh, A., & El-Mowafy, A. (2022a, 23–27 May 2022). The impact of precise inter-satellite ranges on relative precise orbit determination in a smart CubeSats constellation. EGU General Assembly Conference Abstracts, Vienna, Austria. https://doi.org/10.5194/egusphere-egu22-2215
Allahvirdi-Zadeh, A., & El-Mowafy, A. (2022b). CubeSat's attitude determination using GNSS antenna array. International Global Navigation Satellite Systems Conference (IGNSS) 2022, UNSW, Sydney. https://doi.org/10.13140/RG.2.2.29925.68320
Allahvirdi-Zadeh, A., El-Mowafy, A., & Wang, K. (2022). Precise Orbit Determination of CubeSats Using Proposed Observations Weighting Model. In (pp. 1-8). Springer Berlin Heidelberg. https://doi.org/10.1007/1345_2022_160
Allahvirdi-Zadeh, A., Wang, K., & El-Mowafy, A. (2022). Precise Orbit Determination of LEO Satellites Based on Undifferenced GNSS Observations. *Journal of surveying engineering*, *148*(1), 03121001. https://doi.org/10.1061/(ASCE)SU.1943-5428.0000382
Arnold, D., Peter, H., Mao, X., Miller, A., & Jäggi, A. (2023). Precise orbit determination of Spire nano satellites. *Advances in Space Research*, *72*(11), 5030-5046. https://doi.org/10.1016/j.asr.2023.10.012
Barry, C., & Weiss, M. (2022). Alternative Position, Navigation and Timing (A-PNT) Using Time Difference of Arrival (TDOA) of Low Earth Orbit (LEO) Signals Of Opportunity (SOOP). http://hdl.handle.net/10150/666956
Carrere, L., Lyard, F., Cancet, M., & Guillot, A. (2015, April 01, 2015). *FES 2014, a new tidal model on the global ocean with enhanced accuracy in shallow seas and in the Arctic region* https://ui.adsabs.harvard.edu/abs/2015EGUGA..17.5481C
Dach, R., Lutz, S., Walser, P., & Fridez, P. (2015). *Bernese GNSS Software Version 5.2*. Bern Open Publishing. https://doi.org/10.7892/boris.72297
El-Mowafy, A., Wang, K., Li, Y., & Allavirdizadeh, A. (2023). The Impact of Orbital and Clock Errors on Positioning from LEO Constellations and Proposed Orbital Solutions. The ISPRS Geospatial Week-Egypt GSW'2023".
Folkner, W. M., Williams, J. G., & Boggs, D. H. (2009). The planetary and lunar ephemeris DE 421. *IPN progress report*, *42*(178), 1.
González, A., Rodriguez, I., Navarro, P., Sobrero, F., Carbonell, E., Calle, D., & Fernández, J. (2022). Leo satellites for PNT, the next step for precise positioning applications. Proceedings of the 35th International Technical Meeting of the Satellite Division of The Institute of Navigation (ION GNSS+ 2022). https://doi.org/10.33012/2022.18436
Guan, M., Xu, T., Gao, F., Nie, W., & Yang, H. (2020). Optimal Walker Constellation Design of LEO-Based Global Navigation and Augmentation System. *Remote Sensing*, *12*(11).
Guo, F., Yang, Y., Ma, F., Zhu, Y., Liu, H., & Zhang, X. (2023). Instantaneous velocity determination and positioning using Doppler shift from a LEO constellation. *Satellite Navigation*, *4*(1), 9. https://doi.org/10.1186/s43020-023-00098-2
Hauschild, A., Montenbruck, O., Steigenberger, P., Martini, I., & Fernandez-Hernandez, I. (2022). Orbit determination of Sentinel-6A using the Galileo high accuracy service test signal. GPS solutions, 26(4), 120. https://doi.org/10.1007/s10291-022-01312-5
Hong, J., Tu, R., Zhang, P., Zhang, R., Han, J., Fan, L., Wang, S., & Lu, X. (2023). GNSS rapid precise point positioning enhanced by low Earth orbit satellites. *Satellite Navigation*, *4*(1), 11. https://doi.org/10.1186/s43020-023-00100-x
Jäggi, A., Hugentobler, U., & Beutler, G. (2006). Pseudo-Stochastic Orbit Modeling Techniques for Low-Earth Orbiters. *Journal of Geodesy*, *80*(1), 47-60. https://doi.org/10.1007/s00190-006-0029-9
Jardak, N., & Jault, Q. (2022). The Potential of LEO Satellite-Based Opportunistic Navigation for High Dynamic Applications. *Sensors*, *22*(7). https://doi.org/10.3390/s22072541
Kassas, Z. M., Ghadiok, V., & Humphreys, T. E. (2014). Adaptive estimation of signals of opportunity. Proceedings of the 27th International Technical Meeting of the Satellite Division of The Institute of Navigation (ION GNSS+ 2014).
Khalife, J., Neinavaie, M., & Kassas, Z. M. (2020, 20-23 April 2020). Navigation With Differential Carrier Phase Measurements From Megaconstellation LEO Satellites. 2020 IEEE/ION Position, Location and Navigation Symposium (PLANS). https://doi.org/10.1109/PLANS46316.2020.9110199
Pavlis, N., Kenyon, S., Factor, J., & Holmes, S. (2008). Earth gravitational model 2008. In *SEG Technical Program Expanded Abstracts 2008* (pp. 761-763). Society of Exploration Geophysicists. https://doi.org/10.1190/1.3063757
Petit, G., & Luzum, B. (2010). *IERS conventions* (3-89888-989-6) https://www.iers.org/IERS/EN/Publications/TechnicalNotes/tn36.html
Pinell, C., Prol, F. S., Bhuiyan, M. Z. H., & Praks, J. (2023). Receiver architectures for positioning with low earth orbit satellite signals: a survey. *EURASIP Journal on Advances in Signal Processing*, *2023*(1), 60. https://doi.org/10.1186/s13634-023-01022-1

 International Technical Meeting of The Institute of Navigation, Long Beach, California, 23 Jan 2024 - 25 Jan 2024. Proceedings of the 2024 International Technical Meeting of The Institute of Navigation. Institute of Navigation. 756-769. 15 Feb 2024; https://doi.org/10.33012/2024.19485

Prol, F. S., Ferre, R. M., Saleem, Z., Välisuo, P., Pinell, C., Lohan, E. S., Elsanhoury, M., Elmusrati, M., Islam, S., Çelikbilek, K., Selvan, K., Yliaho, J., Rutledge, K., Ojala, A., Ferranti, L., Praks, J., Bhuiyan, M. Z. H., Kaasalainen, S., & Kuusniemi, H. (2022). Position, Navigation, and Timing (PNT) Through Low Earth Orbit (LEO) Satellites: A Survey on Current Status, Challenges, and Opportunities. *IEEE Access*, *10*, 83971-84002. https://doi.org/10.1109/ACCESS.2022.3194050

Schaer, S., Villiger, A., Arnold, D., Dach, R., Prange, L., & Jäggi, A. (2021). The CODE ambiguity-fixed clock and phase bias analysis products: generation, properties, and performance. *Journal of Geodesy*, *95*(7), 81 (81-25). https://doi.org/10.1007/s00190-021-01521-9

Spirent. (2022). SimGEN® Software User Manual for version v8.01.00. Software for the Spirent range of satellite navigation simulator products. In: Spirent Communications PLC England, UK.

Wang, K., Allahvirdi-Zadeh, A., El-Mowafy, A., & Gross, J. N. (2020). A Sensitivity Study of POD Using Dual-Frequency GPS for CubeSats Data Limitation and Resources. *Remote Sensing*, 12(13):2107. https://doi.org/10.3390/rs12132107

Wang, K., & El-Mowafy, A. (2020). Proposed Orbital Products for Positioning Using Mega-Constellation LEO Satellites. *Sensors*, *20*(20), 5806. https://doi.org/10.3390/s20205806

Wang, K., & El-Mowafy, A. (2021). LEO satellite clock analysis and prediction for positioning applications. *Geo-spatial Information Science*, 1-20. https://doi.org/10.1080/10095020.2021.1917310

 International Technical Meeting of The Institute of Navigation, Long Beach, California, 23 Jan 2024 - 25 Jan 2024. Proceedings of the 2024 International Technical Meeting of The Institute of Navigation. Institute of Navigation. 756-769. 15 Feb 2024; https://doi.org/10.33012/2024.19485